

Table III. Fractional Atomic Coordinates with Esd's in Parentheses

atom	x/a	y/b	z/c
Cu	0.4828 (1)	0.59922 (8)	0.5466 (1)
Fe(1)	0.3235 (2)	0.1584 (1)	0.0529 (1)
Fe(2)	0.2021 (1)	0.9003 (1)	0.4295 (1)
S(1)	0.6773 (2)	0.5173 (2)	0.5592 (2)
P(1)	0.6370 (2)	0.5572 (2)	0.4007 (2)
N(1)	0.5271 (6)	0.3884 (5)	0.2915 (6)
N(2)	0.5547 (7)	0.4754 (6)	0.2754 (7)
N(3)	0.4584 (7)	0.6798 (5)	0.4246 (7)
N(4)	0.5578 (7)	0.6675 (5)	0.3895 (7)
C(1)	0.5136 (8)	0.3116 (7)	0.2010 (8)
C(2)	0.487 (1)	0.4993 (9)	0.152 (1)
C(3)	0.3615 (9)	0.7264 (7)	0.3581 (9)
C(4)	0.581 (1)	0.748 (1)	0.358 (2)
C(11)	0.4744 (7)	0.2209 (5)	0.1986 (7)
C(12)	0.3919 (7)	0.2093 (5)	0.2438 (7)
C(13)	0.3736 (7)	0.1064 (5)	0.2115 (7)
C(14)	0.4448 (7)	0.0545 (5)	0.1462 (7)
C(15)	0.5070 (7)	0.1252 (5)	0.1383 (7)
C(21)	0.2320 (9)	0.2548 (6)	-0.0665 (9)
C(22)	0.2790 (9)	0.1677 (6)	-0.1285 (9)
C(23)	0.2286 (9)	0.0846 (6)	-0.1299 (9)
C(24)	0.1505 (9)	0.1204 (6)	-0.0688 (9)
C(25)	0.1526 (9)	0.2255 (6)	-0.0296 (9)
C(31)	0.2585 (5)	0.7551 (5)	0.3894 (5)
C(32)	0.2609 (5)	0.7802 (5)	0.5113 (5)
C(33)	0.1405 (5)	0.8152 (5)	0.4977 (5)
C(34)	0.0636 (5)	0.8117 (5)	0.3674 (5)
C(35)	0.1365 (5)	0.7746 (5)	0.3005 (5)
C(41)	0.3160 (8)	0.9825 (7)	0.4214 (9)
C(42)	0.3155 (8)	1.0107 (7)	0.5421 (9)
C(43)	0.1938 (8)	1.0443 (7)	0.5246 (9)
C(44)	0.1189 (8)	1.0368 (7)	0.3932 (9)
C(45)	0.1945 (8)	0.9986 (7)	0.3293 (9)
C(51)	0.7704 (7)	0.5703 (5)	0.3883 (6)
C(52)	0.7905 (7)	0.5179 (5)	0.2834 (6)
C(53)	0.8979 (7)	0.5267 (5)	0.2776 (6)
C(54)	0.9851 (7)	0.5880 (5)	0.3768 (6)
C(55)	0.9650 (7)	0.6404 (5)	0.4817 (6)
C(56)	0.8576 (7)	0.6316 (5)	0.4874 (6)
S(2)	0.2668 (4)	0.7593 (4)	0.0049 (4)
C(5)	0.144 (1)	0.802 (1)	-0.111 (1)
O(1)	0.331 (1)	0.8384 (7)	0.104 (1)
O(2)	0.344 (1)	0.6825 (9)	-0.035 (1)
O(3)	0.201 (2)	0.716 (1)	0.047 (2)
F(1)	0.070 (1)	0.733 (1)	-0.197 (1)
F(2)	0.075 (1)	0.874 (1)	-0.071 (2)
F(3)	0.189 (2)	0.840 (2)	-0.169 (2)
C(s)	0.051 (2)	0.512 (2)	0.060 (2)
O(s)	0.177 (3)	0.516 (2)	0.072 (3)

Crystallographic Studies. Crystals of **3** suitable for X-ray diffraction were obtained at room temperature from a saturated ethanol solution. Data were collected on an Enraf-Nonius CAD4 diffractometer. Cell constants were obtained by the least-squares refinement of the setting angles of 25 reflections in the range $24^\circ < 2\theta(\text{Mo K}\alpha_1) < 28^\circ$. The space group was determined by careful examination of systematic extinctions in the listing of the measured reflections. Data reductions were carried out using the SDP crystallographic computing package.¹⁴ Table II presents further crystallographic information.

The structure was solved and refined using a combination of the SDP crystallographic computing package¹⁴ and the SHELX-76 package.¹⁵ The position of Fe, S, and P atoms was determined by direct methods. All remaining non-hydrogen atoms were located by the usual combination of full-matrix least-squares refinement and difference electron density syntheses. The compound crystallizes with half a molecule of ethanol per unit cell. The CF_3SO_3 group was found to be highly disordered. No splitting model was successful. We finally constrained the C-F, S-O, F-F, and O-O bond lengths to 1.33, 1.43, 2.16, and 2.33 Å, respectively, and we took the high anisotropic values, since the rest of the structure refined nicely. Atomic scattering factors were taken from the usual tabulations.¹⁶ Anomalous dispersion terms for Fe, S, and P atoms were

included in F_c .¹⁷ An empirical absorption correction was applied.¹⁸ The final refinements were conducted using the SHELX-76 program. All non-hydrogen atoms were allowed to vibrate anisotropically, except carbon atoms of the phenyl and cyclopentadienyl rings which were refined as isotropic rigid groups in order to reduce the number of variable parameters (C_6H_5 ring, C-C = 1.395 Å; C_5H_5 and C_5H_4 rings, C-C = 1.420 Å). Hydrogen atoms were entered in idealized positions (C-H = 0.97 Å) and held fixed during refinements. Scattering factors for the hydrogen atoms were taken from Stewart et al.¹⁹

Final atomic coordinates for non-hydrogen atoms are given in Table III. Structure amplitudes ($10|F_o|$ vs $10|F_c|$) are available as Table S1.²⁰ Table S2 lists the anisotropic thermal parameters ($\times 100$).²⁰ Table S3 lists the isotropic thermal parameters ($\times 100$).²⁰

Acknowledgment. We thank Dr. D. de Montauzon for electrochemical measurements and for fruitful discussions.

Supplementary Material Available: Table S2, giving anisotropic thermal parameters for compound **3**, and Table S3, giving isotropic thermal parameters for compound **3** (2 pages); Table S1, listing structure factor amplitudes ($\times 10$) for compound **3** (18 pages). Ordering information is given on any current masthead page.

- (16) Cromer, D. T.; Waber, J. T. *International Tables for X-ray Crystallography*; Kynoch Press: Birmingham, England, 1974; Vol. 4, Table 2.2B.
- (17) Cromer, D. T.; Waber, J. T. *International Tables for X-ray Crystallography*; Kynoch Press: Birmingham, England, 1974; Vol. 4, Table 2.3.1.
- (18) North, A. C. T.; Phillips, D. C.; Mathews, F. S. *Acta Crystallogr.* **1968**, *A24*, 351.
- (19) Stewart, R. F.; Davidson, E. R.; Simpson, W. T. *J. Chem. Phys.* **1965**, *42*, 3175.
- (20) See paragraph at end of paper regarding supplementary material.

Contribution from the CNR, Centro di Studio sulla Sintesi e la Struttura dei Composti dei Metalli di Transizione nei Bassi Stati di Ossidazione, and Dipartimento di Chimica Inorganica e Metallorganica, Università di Milano, Milano, Italy, and Istituto di Chimica Strutturistica Inorganica, Università di Milano, Via G. Venezian 21, 20133 Milano, Italy

Mixed Platinum-Rhodium Carbonyl Clusters. The Isolation of $[\text{Pt}_4\text{Rh}_{18}(\text{CO})_{35}]^{4+}$, an Example of a Cherry-like Cluster with a Semiexposed Tetraplatinum Core

Alessandro Fumagalli,^{*1a} Secondo Martinengo,^{1b} Gianfranco Ciani,^{1c} Norberto Masciocchi,^{1c} and Angelo Sironi^{*1c}

Received June 5, 1991

Our previous studies of Pt-Rh mixed clusters led to the isolation of several carbonyl anions²⁻⁷ which contain platinum as the minor component of the metal skeleton. Partitioning these species into classes according to the size, we have the small clusters such as $[\text{PtRh}_4(\text{CO})_{14}]^{2-}$,^{2,3} $[\text{PtRh}_4(\text{CO})_{12}]^{2-}$,^{2,3} $[\text{PtRh}_5(\text{CO})_{15}]^{2-}$,² and $[\text{PtRh}_6(\text{CO})_{16}]^{2-}$,⁴ whose structures consist of simple polyhedra where the Pt atom has a metallic connectivity of 3 or 4. With the species of intermediate size, such as $[\text{PtRh}_8(\text{CO})_{19}]^{2-}$ ⁵ and $[\text{Pt}_2\text{Rh}_9(\text{CO})_{22}]^{3-}$,⁶ the tendency of the Pt atom(s) to occupy the

- (14) *Enraf-Nonius Structure Determination Package*, 4th ed.; Frenz B. A. & Associates, Inc.: College Station, TX; Enraf-Nonius: Delft, The Netherlands, 1981.
- (15) Sheldrick, G. M. *SHELX-76, Program for Crystal Structure Determination*; University of Cambridge: Cambridge, England, 1976.

- (1) (a) CNR. (b) Dipartimento di Chimica Inorganica e Metallorganica, Università di Milano. (c) Istituto di Chimica Strutturistica Inorganica, Università di Milano.
- (2) Fumagalli, A.; Martinengo, S.; Chini, P.; Galli, D.; Heaton, B. T.; Della Pergola, R. *Inorg. Chem.* **1984**, *23*, 2947.
- (3) Fumagalli, A.; Martinengo, S. *Inorg. Synth.* **1989**, *26*, 372.
- (4) Fumagalli, A.; Martinengo, S.; Galli, D.; Albinati, A.; Ganazzoli, F. *Inorg. Chem.* **1989**, *28*, 2476.
- (5) Fumagalli, A.; Martinengo, S.; Ciani, G.; Marturano, G. *Inorg. Chem.* **1986**, *25*, 592.
- (6) Fumagalli, A.; Martinengo, S.; Ciani, G. *J. Organomet. Chem.* **1984**, *273*, C46.
- (7) Fumagalli, A.; Martinengo, S.; Ciani, G. *J. Chem. Soc., Chem. Commun.* **1983**, 1381.

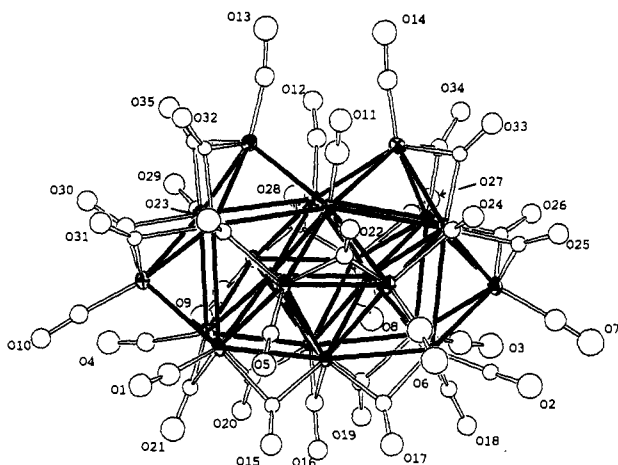


Figure 1. ORTEP drawing of the anion $[\text{Pt}_4\text{Rh}_{18}(\text{CO})_{35}]^{4-}$, with partial labeling scheme. Thermal ellipsoids have been drawn at the 30% probability level.

sites of higher metallic connectivity (6–7) within the more complex cluster frameworks can be clearly recognized. In the high nuclearity species $[\text{PtRh}_{12}(\text{CO})_{24}]^{4-7}$ and $[\text{Pt}_2\text{Rh}_{11}(\text{CO})_{24}]^{3-7}$ one Pt atom is fully encapsulated in a 12-metal cage.

The tendency of the heavier metal to occupy, within the metal skeleton, the inner sites of higher metallic connectivity appears recurrent in all bimetallic systems, where the cluster growth, a process induced chemically or thermally, generally proceeds with gradual encapsulation of the heaviest metal, toward complete segregation. This situation is reminiscent of that found in the "cherry" crystallites⁸ and is very likely the result of the balance of M–CO and M–M bonding energies which, on going from the first to the third transition, increasingly favors M–M rather than M–CO interactions.⁹

Several high-nuclearity clusters with a completely segregated metal core have been so far reported, from $[\text{PtRh}_{12}(\text{CO})_{24}]^{4-}$, which can be considered the minimal term, up to the giant $[\text{Pt}_6\text{Ni}_{38}(\text{CO})_{48}\text{H}_x]^{5-10}$ where an octahedral Pt_6 core is fully encapsulated in an heterometallic matrix. The title compound, $[\text{Pt}_4\text{Rh}_{18}(\text{CO})_{35}]^{4-}$, is the first example which shows a small three-dimensional Pt cluster halfway toward full encapsulation in an heterometal matrix, thus representing a significative step in the growing sequence which ideally would lead to the larger cherry-like clusters.

Results and Discussion

The tetraanion $[\text{Pt}_4\text{Rh}_{18}(\text{CO})_{35}]^{4-}$ was isolated for the first time from the mixture of cluster anions obtained by the pyrolysis of $\text{Na}[\text{PtRh}_5(\text{CO})_{15}]$ in methanol at reflux, a reaction intended to produce $[\text{Pt}_2\text{Rh}_{11}(\text{CO})_{24}]^{3-}$. Separation of the mixture components was achieved by fractional precipitation from water of the alkali-metal salts induced by addition of suitable amounts of the Na^+ , K^+ , and Cs^+ halides (in the given order); in this way anions with increasing C/M (charge/metal) ratios are precipitated sequentially.^{9,11} After the separation of a fraction containing essentially the Cs^+ salt of $[\text{Pt}_2\text{Rh}_{11}(\text{CO})_{24}]^{3-}$, treatment with acetic acid of the mother liquor, which contained anions with higher C/M ratios such as $[\text{Pt}_2\text{Rh}_9(\text{CO})_{22}]^{3-}$, gave, within a few hours, a microcrystalline precipitate of the cesium salt of the title compound.

$[\text{Pt}_4\text{Rh}_{18}(\text{CO})_{35}]^{4-}$ was also isolated in lower yields when we attempted the synthesis of $[\text{Pt}_2\text{Rh}_9(\text{CO})_{22}]^{3-}$ by reaction of $[\text{PtRh}_5(\text{CO})_{15}]^-$ and $[\text{PtRh}_4(\text{CO})_{12}]^{2-}$ as $[\text{PPN}]^+$ salts in MeCN. The slow reaction at room temperature of the two anions yielded a mixture which was converted to the Na^+ salts and worked up with the above-mentioned technique in water. After separation of a

Table I. Relevant Bond Distances (Å) and Angles (deg) within the Anion $[\text{Pt}_4\text{Rh}_{18}(\text{CO})_{35}]^{4-}$

Pt1–Pt2	2.559 (1)		
Pt3–Pt4	2.827 (2)		
Pt1–Pt3	2.708 (2)		
Pt2–Pt3	2.704 (2)		
Pt2–Pt4	2.697 (2)		
Pt1–Pt4	2.690 (2)		
Pt1–Rh1	2.684 (3)	Pt3–Rh7	2.831 (3)
Pt1–Rh2	2.779 (3)	Pt3–Rh8	2.806 (3)
Pt1–Rh5	2.787 (3)	Pt3–Rh13	3.042 (2)
Pt1–Rh6	2.673 (2)	Pt3–Rh14	3.040 (2)
Pt1–Rh7	3.084 (3)	Pt3–Rh17	2.834 (3)
Pt1–Rh11	3.140 (3)	Pt3–Rh18	2.867 (3)
Pt1–Rh12	3.344 (2)		
Pt1–Rh13	2.678 (3)		
Pt1–Rh16	2.683 (3)		
Pt2–Rh2	2.768 (3)	Pt4–Rh10	2.812 (3)
Pt2–Rh3	2.683 (3)	Pt4–Rh11	2.834 (3)
Pt2–Rh4	2.663 (3)	Pt4–Rh15	3.046 (2)
Pt2–Rh5	2.787 (2)	Pt4–Rh16	3.027 (2)
Pt2–Rh8	3.056 (2)	Pt4–Rh17	2.873 (3)
Pt2–Rh9	3.356 (2)	Pt4–Rh18	2.851 (3)
Pt2–Rh10	3.159 (3)		
Pt2–Rh14	2.677 (2)		
Pt2–Rh15	2.680 (2)		
Rh1–Rh2	2.778 (3)	Rh2–Rh7	2.971 (3)
Rh2–Rh3	2.777 (3)	Rh2–Rh8	2.977 (3)
Rh4–Rh5	2.772 (3)	Rh5–Rh10	2.986 (3)
Rh5–Rh6	2.777 (3)	Rh5–Rh11	3.009 (4)
Rh1–Rh7	2.835 (3)	Rh13–Rh12	2.729 (3)
Rh3–Rh8	2.830 (4)	Rh14–Rh9	2.734 (4)
Rh4–Rh10	2.844 (4)	Rh15–Rh9	2.728 (4)
Rh6–Rh11	2.808 (3)	Rh16–Rh12	2.719 (3)
Rh1–Rh12	2.817 (3)	Rh13–Rh7	2.675 (3)
Rh3–Rh9	2.794 (3)	Rh14–Rh8	2.660 (3)
Rh4–Rh9	2.792 (3)	Rh15–Rh10	2.697 (3)
Rh6–Rh12	2.794 (4)	Rh16–Rh11	2.687 (4)
Rh1–Rh13	3.167 (4)	Rh13–Rh17	2.719 (4)
Rh3–Rh14	3.171 (4)	Rh14–Rh18	2.714 (4)
Rh4–Rh15	3.079 (4)	Rh15–Rh18	2.711 (4)
Rh6–Rh16	3.142 (4)	Rh16–Rh17	2.711 (3)
Rh1–Rh6	2.889 (4)	Rh7–Rh8	2.688 (3)
Rh3–Rh4	2.888 (4)	Rh10–Rh11	2.698 (3)
Rh2–Rh5	2.917 (3)		
Rh13–Rh16	2.937 (4)	Rh17–Rh18	3.890 (4)
Rh14–Rh15	2.952 (4)		

	av	min	max
M–C _{ter}	1.81	1.72 (4)	1.89 (4)
C _{ter} –O _{ter}	1.18	1.11 (5)	1.30 (4)
M–C _{ter} –O _{ter}	173	169 (4)	177 (4)
M–C _{brd}	2.00	1.91 (3)	2.15 (3)
C _{brd} –O _{brd}	1.20	1.13 (3)	1.26 (3)
M–C _{brd} –O _{brd}	137	126 (3)	152 (2)

first potassic fraction precipitated at ca. 20% KBr concentration, a second fraction was obtained by saturation with KBr. Redissolution of this fraction in water, followed by addition of NaCl up to 10% concentration gave, after 24 h, precipitation of a product whose IR spectrum was identical to that of the first synthesis. Metathesis with $[\text{NET}_4]^+$ and recrystallization from acetone/2-propanol, yielded crystals which were characterized by single-crystal X-ray diffraction as $[\text{NET}_4]_4[\text{Pt}_4\text{Rh}_{18}(\text{CO})_{35}] \cdot \text{acetone}$.

The IR spectra of the alkaline (Na^+ , Cs^+) salts in THF have bands at 2005 s, 1865 mw, 1843 m, and 1827 ms cm^{-1} . In CH_3CN and acetone both the alkaline and the $[\text{NET}_4]^+$ salts show the same spectra with bands at 2000 s, 1858 m, 1815 sh, and 1788 w cm^{-1} .

The crystal structure of $[\text{NET}_4]_4[\text{Pt}_4\text{Rh}_{18}(\text{CO})_{35}] \cdot \text{acetone}$ consists of an ionic packing of the cluster anions $[\text{Pt}_4\text{Rh}_{18}(\text{CO})_{35}]^{4-}$, the $[\text{NET}_4]^+$ cations, and clathrate acetone molecules, with normal van der Waals interactions.

The structure of the tetraanion is shown in Figure 1, and relevant bond distances and angles are given in Table I. The

(8) Sachtler, W. M. H.; Van Santen, R. A. *Adv. Catal.* 1977, 26, 69.

(9) Chini, P.; Longoni, G.; Albano, V. G. *Adv. Organomet. Chem.* 1976, 14, 311–312.

(10) Ceriotti, A.; Demartin, F.; Longoni, G.; Manassero, M.; Marchionna, M.; Piva, G.; Sansoni, M. *Angew. Chem., Int. Ed. Engl.* 1985, 24, 697.

(11) Martinengo, S.; Fumagalli, A. Unpublished results.

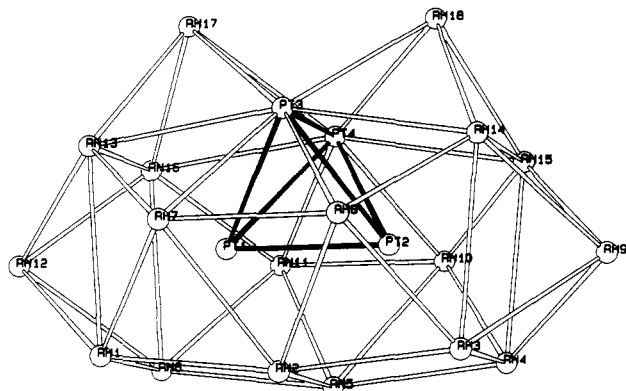


Figure 2. Bare $\text{Pt}_4\text{Rh}_{18}$ cluster with atom-numbering scheme.

overall idealized symmetry is C_{2v} with the 2-fold axis passing through the midpoints of the Pt3–Pt4 and Rh2–Rh5 edges and through the C16–O16 carbonyl.

The inner part of the metallic frame is a distorted tetrahedron of Pt atoms, with bonding distances in the range 2.559 (1)–2.827 (2) Å, and average value of 2.698 Å. With reference to the drawing of the naked metal skeleton reported in Figure 2, it can be seen that the longer distance corresponds to the "outer" Pt–Pt contact, while the Pt1–Pt2 distance (2.559 (1) Å), which connects the two atoms encapsulated in the metallic frame, is considerably shorter than the distance in the bulk (2.774 Å), as well as that found in $[\text{Pt}_2\text{Rh}_9(\text{CO})_{22}]^{3-}$ (2.812 (2) Å), where the Pt–Pt interaction is also internal to the cluster. Eighteen Rh atoms surround the Pt tetrahedron, yielding a cage very similar to that found in the homometallic $[\text{Rh}_{22}(\text{CO})_{35}\text{H}_x]^{5-}$.¹² This is not surprising, since the metal skeleton of all the known mixed Pt–Rh clusters always have a structural correspondence in some iso-electronic homometallic Rh derivative.¹³ Very likely this is due to the high Rh/Pt ratio, which makes the Rh atoms prevailing in addressing the cage structure. The metallic structure can be described as a slightly distorted body-centered cubic framework. Alternatively, in keeping with the description reported for $[\text{Rh}_{22}(\text{CO})_{35}\text{H}_x]^{5-}$,¹² the metal skeleton can be envisaged as derived from the fusion of two platinum-centered metallic cubes (thus generating a tetragonal prism) which has been capped on all but two adjacent faces by μ_4 -Rh atoms.

The Rh–Rh interactions range from 2.660 (3) Å (Rh8–Rh14) to 3.167 (4) Å (Rh3–Rh14), and can be divided, following the topology and the idealized symmetry of the metal cage, into several distinct groups, as reported in Table I. The Rh17–Rh18 distance of 3.890 (3) Å clearly indicates that no bond is occurring, while the analogous interactions for the other two adjacent Rh caps (Rh7–Rh8 and Rh10–Rh11) definitely show bonding values of 2.688 (3) and 2.698 (3) Å, respectively.

The Pt–Rh distances range from 2.663 (3) Å (Pt2–Rh4) to 3.356 (3) Å (Pt2–Rh9), with an average value of 2.871 Å; interactions above 3.50 Å were excluded from this analysis. Considerably lower mean values, 2.707, 2.790, 2.776, and 2.730 Å, were found in $[\text{Pt}_2\text{Rh}_9(\text{CO})_{22}]^{3-}$, $[\text{PtRh}_5(\text{CO})_{15}]^-$, $[\text{PtRh}_{12}(\text{CO})_{24}]^{4-}$ and $[\text{PtRh}_8(\text{CO})_{19}]^{2-}$, respectively. A closer average value was found in $[\text{PtRh}_6(\text{CO})_{16}]^{2-}$ (2.879 Å), where the Pt atom is externally coordinated to the Rh_6 octahedron via one long (3.167 (2) Å) and two short (mean 2.735 Å) interactions.

Fourteen, out of 35, carbonyl ligands are terminally bonded to the metal cluster, two on the surface Pt atoms and 12 on the Rh atoms with the lowest metallic connectivity. The remaining 21 carbonyls are μ_2 -coordinated on Rh–Rh edges. The carbonyl

Table II. Summary of Crystal Data for $[\text{NEt}_4]_4[\text{Pt}_4\text{Rh}_{18}(\text{CO})_{35}] \cdot \text{acetone}$

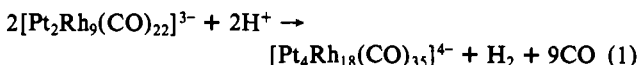
chem formula	$\text{C}_{70}\text{H}_{86}\text{N}_4\text{O}_{36}\text{Pt}_4\text{Rh}_{18}$
fw	4192.12
syst	orthorhombic
space group	$P2_12_12_1$ (No. 19)
a, Å	12.914 (9)
b, Å	27.196 (15)
c, Å	28.378 (12)
V, Å ³	9967 (17)
Z	4
D_c , g·cm ⁻³	2.794
F(000)	7796
T, °C	22
radiation	Mo K α ($\lambda = 0.71073$ Å)
μ (Mo K α), cm ⁻¹	85.72
no. of reflns having $I > 2\sigma(I)$	4765
R	0.043 ^a
R_w	0.044 ^b
esd	1.360

$$^a R = \sum |F_o - k|F_c| / \sum F_o. \quad ^b R_w = [\sum w(F_o - k|F_c|)^2 / \sum wF_o^2]^{1/2}.$$

distribution around the $\text{Pt}_4\text{Rh}_{18}$ metallic frame can be related to the CO disposition in $[\text{Rh}_{14}(\text{CO})_{25}]^{4-}$.¹⁴ In fact, ideal compenetration of two such M_{14} units would lead to a M_{22} frame. If we imagine performing this operation with elimination of the carbonyl ligands belonging to the atoms going to be shared, the resulting topology exactly matches that of $[\text{Pt}_4\text{Rh}_{18}(\text{CO})_{35}]^{4-}$. This carbonyl stereochemistry is however different from that observed in $[\text{Rh}_{22}(\text{CO})_{35}\text{H}_x]^{5-}$; the most relevant difference in the present compound is the lack of face-bridging μ_3 -carbonyls. The terminal CO distances span the range from 1.11 (5) to 1.30 (4) Å, with an average value of 1.18 Å. The corresponding values for the μ_2 -bridging carbonyls, none of which shows extreme asymmetry, are 1.13 (3), 1.26 (3), and 1.20 Å.

The product does not appear as an hydride because ¹H NMR spectroscopy of the cesium salt in acetone-*d*₆ at -90°C gave no detectable hydrido signal and space-filling models exclude hydrogen coordination on the metal surface. Moreover, the lack of reaction with excess Na_2CO_3 in THF also excludes the presence of labile hydrides. The formal electron count for this anion thus gives 276 cluster valence electrons (CVE), in agreement with rule 7 of the generalized polyhedral skeletal electron pair approach¹⁵ ($12n_s + \Delta$, where n_s is the number of surface atoms and Δ is characteristic of the enclosed unit, in this case 60 for the tetrahedron). This leads us to assign three hydrido ligands to the isostructural $[\text{Rh}_{22}(\text{CO})_{35}\text{H}_x]^{5-}$.¹²

The molecular formula and the circumstances in which the compound was isolated suggest a close relation with the elusive $[\text{Pt}_2\text{Rh}_9(\text{CO})_{22}]^{3-}$, from which $[\text{Pt}_4\text{Rh}_{18}(\text{CO})_{35}]^{4-}$ could be generated by hydrolysis in a neutral or a weakly acidic aqueous medium, followed by oxidative condensation, according to the overall reaction



This hypothesis is supported by the fact that $[\text{Pt}_4\text{Rh}_{18}(\text{CO})_{35}]^{4-}$ was obtained with similar low yields and scarce reproducibility from the same alkali-metal fraction of $[\text{Pt}_2\text{Rh}_9(\text{CO})_{22}]^{3-}$, where it is not supposed to be originally present because of the lower C/M ratio. Moreover, the higher yield obtained by addition of acetic acid is consistent with the suggested hydrolytic process.

Experimental Section

All the reactions and subsequent manipulations were carried out under a nitrogen atmosphere. Tetrahydrofuran (THF) was distilled prior to use from sodium benzophenone ketyl; all the other analytical grade

- (12) Vidal, J. L.; Schoening, R. C.; Troup, J. M. *Inorg. Chem.* **1981**, *20*, 227. Notably, in the same crystal the penta- and the tetraanionic $[\text{Rh}_{22}(\text{CO})_{35}\text{H}_x]^{3-}$ and $[\text{Rh}_{22}(\text{CO})_{35}\text{H}_{x+1}]^{4-}$ species are present; for sake of simplicity only the first one will be referred to throughout the paper.
- (13) Another 22-metal Rh cluster, $[\text{Rh}_{22}(\text{CO})_{37}]^{4-}$, is known, but it would allow the presence of a single fully encapsulated platinum atom: Martinengo, S.; Ciani, G.; Sironi, A. *J. Am. Chem. Soc.* **1980**, *102*, 7564.

- (14) (a) Martinengo, S.; Ciani, G.; Sironi, A.; Chini, P. *J. Am. Chem. Soc.* **1978**, *100*, 7096. (b) Ciani, G.; Sironi, A.; Martinengo, S. *J. Chem. Soc., Dalton Trans.* **1982**, 1099.
- (15) Mingos, D. M. P.; May, A. S. In *The Chemistry of Metal Cluster Complexes*; Shriver, D. F., Kaesz, H. D., Adams, R. D., Eds.; VCH: Weinheim, Germany, 1989; p 11.

Table III. Fractional Atomic Coordinates (with Esd's in Parentheses) for the Compound $[\text{NEt}_4]_4[\text{Pt}_4\text{Rh}_{18}(\text{CO})_{35}]\cdot\text{acetone}$

atom	x	y	z	atom	x	y	z
Pt1	0.44267 (9)	0.45641 (3)	0.36434 (4)	C23	0.717 (2)	0.4224 (9)	0.430 (1)
Pt2	0.4176 (1)	0.54837 (4)	0.34894 (4)	O23	0.797 (2)	0.4116 (8)	0.4472 (9)
Pt3	0.52790 (9)	0.52113 (4)	0.42560 (5)	C24	0.653 (2)	0.6326 (9)	0.399 (1)
Pt4	0.31150 (9)	0.50640 (4)	0.42024 (5)	O24	0.728 (2)	0.6535 (7)	0.4134 (9)
Rh1	0.5753 (2)	0.40018 (7)	0.3154 (1)	C25	0.486 (2)	0.6937 (9)	0.365 (1)
Rh2	0.5502 (2)	0.49796 (7)	0.28945 (9)	O25	0.537 (2)	0.7319 (7)	0.3735 (9)
Rh3	0.5203 (2)	0.59881 (8)	0.2825 (1)	C26	0.266 (2)	0.6800 (9)	0.360 (1)
Rh4	0.2990 (2)	0.58396 (8)	0.28017 (9)	O26	0.208 (2)	0.7125 (7)	0.3714 (8)
Rh5	0.3267 (2)	0.48306 (7)	0.28556 (9)	C27	0.126 (3)	0.597 (1)	0.381 (1)
Rh6	0.3538 (2)	0.38582 (7)	0.3128 (1)	O27	0.045 (2)	0.6155 (8)	0.3867 (9)
Rh7	0.6790 (2)	0.47047 (7)	0.3721 (1)	C28	0.094 (3)	0.483 (1)	0.383 (1)
Rh8	0.6504 (2)	0.56706 (7)	0.3568 (1)	O28	0.014 (2)	0.4838 (7)	0.4053 (9)
Rh9	0.3848 (2)	0.66748 (8)	0.3220 (1)	C29	0.188 (2)	0.3900 (9)	0.417 (1)
Rh10	0.1748 (2)	0.53431 (8)	0.3479 (1)	O29	0.123 (2)	0.3701 (7)	0.4394 (9)
Rh11	0.2029 (2)	0.43745 (7)	0.3640 (1)	C30	0.363 (3)	0.323 (1)	0.422 (1)
Rh12	0.4757 (2)	0.33529 (7)	0.3781 (1)	O30	0.329 (2)	0.2896 (7)	0.4483 (8)
Rh13	0.5657 (2)	0.41074 (7)	0.4264 (1)	C31	0.584 (2)	0.3364 (8)	0.425 (1)
Rh14	0.5045 (2)	0.62628 (7)	0.3909 (1)	O31	0.639 (2)	0.3083 (7)	0.4472 (9)
Rh15	0.2786 (2)	0.61109 (7)	0.3851 (1)	C32	0.564 (2)	0.4136 (8)	0.497 (1)
Rh16	0.3405 (2)	0.39601 (7)	0.4229 (1)	O32	0.611 (2)	0.3981 (7)	0.5303 (8)
Rh17	0.4331 (2)	0.45375 (8)	0.48839 (9)	C33	0.482 (2)	0.6502 (9)	0.455 (1)
Rh18	0.3896 (2)	0.59302 (8)	0.4643 (1)	O33	0.507 (2)	0.6841 (7)	0.4800 (9)
C1	0.679 (3)	0.352 (1)	0.305 (1)	C34	0.268 (3)	0.632 (1)	0.450 (1)
O1	0.749 (2)	0.3267 (8)	0.3046 (9)	O34	0.210 (2)	0.6576 (7)	0.4758 (8)
C2	0.582 (2)	0.6508 (9)	0.260 (1)	C35	0.333 (2)	0.4000 (9)	0.491 (1)
O2	0.634 (2)	0.6856 (9)	0.247 (1)	O35	0.293 (2)	0.3797 (7)	0.5222 (9)
C3	0.211 (3)	0.627 (1)	0.259 (2)	N1	0.962 (2)	0.4066 (9)	0.571 (1)
O3	0.137 (2)	0.6564 (9)	0.246 (1)	C111	0.976 (3)	0.429 (1)	0.520 (1)
C4	0.291 (3)	0.325 (1)	0.306 (1)	C112	0.917 (3)	0.479 (1)	0.520 (1)
O4	0.251 (2)	0.2880 (8)	0.308 (1)	C121	1.034 (3)	0.359 (1)	0.575 (1)
C5	0.792 (2)	0.4538 (9)	0.339 (1)	C122	1.000 (3)	0.316 (1)	0.540 (2)
O5	0.866 (2)	0.4449 (8)	0.318 (1)	C131	0.994 (3)	0.441 (1)	0.613 (1)
C6	0.758 (3)	0.591 (1)	0.321 (2)	C132	1.119 (3)	0.457 (1)	0.604 (1)
O6	0.824 (2)	0.6002 (9)	0.298 (1)	C141	0.851 (4)	0.393 (1)	0.580 (2)
C7	0.374 (3)	0.720 (1)	0.282 (1)	C142	0.822 (3)	0.363 (1)	0.624 (2)
O7	0.361 (2)	0.751 (1)	0.255 (1)	N2	0.944 (2)	0.2239 (8)	0.3929 (9)
C8	0.069 (3)	0.540 (1)	0.305 (1)	C211	0.941 (3)	0.271 (1)	0.369 (2)
O8	0.008 (2)	0.5432 (8)	0.277 (1)	C212	0.903 (3)	0.317 (1)	0.401 (1)
C9	0.113 (3)	0.402 (1)	0.330 (1)	C221	0.984 (4)	0.195 (1)	0.359 (2)
O9	0.058 (2)	0.3766 (8)	0.3049 (9)	C222	0.977 (4)	0.135 (2)	0.371 (2)
C10	0.492 (3)	0.271 (1)	0.356 (1)	C231	0.990 (4)	0.220 (1)	0.441 (2)
O10	0.497 (2)	0.2323 (7)	0.3393 (8)	C232	1.117 (4)	0.231 (1)	0.431 (2)
C11	0.591 (3)	0.536 (1)	0.479 (2)	C241	0.825 (4)	0.211 (1)	0.408 (2)
O11	0.647 (2)	0.5439 (7)	0.5104 (9)	C242	0.755 (3)	0.211 (1)	0.358 (2)
C12	0.218 (3)	0.516 (1)	0.471 (1)	N3	0.893 (2)	0.6497 (8)	0.571 (1)
O12	0.164 (2)	0.5165 (7)	0.5021 (8)	C311	0.882 (3)	0.614 (1)	0.532 (2)
C13	0.422 (3)	0.477 (1)	0.545 (1)	C312	0.944 (4)	0.625 (2)	0.487 (2)
O13	0.416 (2)	0.4842 (8)	0.588 (1)	C321	0.870 (3)	0.705 (1)	0.555 (2)
C14	0.388 (3)	0.592 (1)	0.525 (1)	C322	0.751 (4)	0.704 (1)	0.537 (2)
O14	0.377 (2)	0.5952 (8)	0.567 (1)	C331	1.004 (4)	0.654 (1)	0.583 (2)
C15	0.633 (2)	0.4431 (9)	0.261 (1)	C332	1.048 (4)	0.606 (2)	0.605 (2)
O15	0.692 (2)	0.4381 (7)	0.2307 (9)	C341	0.823 (4)	0.634 (2)	0.616 (2)
C16	0.451 (2)	0.481 (1)	0.242 (1)	C342	0.821 (4)	0.671 (1)	0.656 (2)
O16	0.456 (2)	0.4778 (7)	0.1984 (8)	N4	0.098 (3)	0.2670 (9)	0.163 (1)
C17	0.604 (2)	0.5468 (9)	0.246 (1)	C411	0.219 (7)	0.289 (2)	0.136 (3)
O17	0.653 (2)	0.5498 (8)	0.212 (1)	C412	0.248 (6)	0.281 (2)	0.187 (3)
C18	0.411 (2)	0.6097 (9)	0.234 (1)	C421	0.049 (5)	0.303 (2)	0.200 (2)
O18	0.397 (2)	0.6225 (7)	0.1968 (8)	C422	-0.064 (5)	0.301 (2)	0.213 (2)
C19	0.251 (3)	0.526 (1)	0.238 (1)	C431	0.044 (5)	0.287 (2)	0.119 (3)
O19	0.212 (2)	0.5217 (7)	0.2022 (8)	C432	0.062 (5)	0.245 (2)	0.090 (2)
C20	0.279 (2)	0.422 (1)	0.259 (1)	C441	0.044 (4)	0.218 (2)	0.177 (2)
O20	0.230 (2)	0.4063 (7)	0.2248 (8)	C442	0.073 (5)	0.211 (2)	0.224 (3)
C21	0.470 (2)	0.3653 (9)	0.273 (1)	OS	0.903 (3)	0.410 (1)	0.133 (1)
O21	0.483 (2)	0.3438 (8)	0.238 (1)	CS1	0.902 (4)	0.456 (1)	0.158 (2)
C22	0.758 (2)	0.5308 (9)	0.397 (1)	CS2	0.150 (3)	0.992 (1)	0.365 (2)
O22	0.826 (2)	0.5397 (6)	0.4243 (8)	CS3	-0.017 (4)	0.454 (2)	0.195 (2)

solvents, water, and aqueous solutions were degassed in vacuum and stored under nitrogen. $\text{Na}[\text{PtRh}_5(\text{CO})_{15}]$, $[\text{PPN}][\text{PtRh}_5(\text{CO})_{15}]$, and $[\text{PPN}]_2[\text{PtRh}_4(\text{CO})_{14}]$ were prepared according to the literature.^{2,3} Infrared spectra were recorded on a Perkin-Elmer 781 grating spectrophotometer using 0.1-mm calcium fluoride cells previously purged with nitrogen.

Synthesis of $[\text{Pt}_4\text{Rh}_{18}(\text{CO})_{35}]^{4-}$. (a) **Synthesis as a Byproduct of the Synthesis of $[\text{Pt}_2\text{Rh}_{11}(\text{CO})_{24}]^{3-}$.** According to the reported procedure,² $\text{RhCl}_3 \cdot x\text{H}_2\text{O}$ (39% Rh; 4.385 g, 16.62 mmol) and anhydrous Na_2PtCl_6 (1.372 g, 3.023 mmol) were submitted to reductive carbonylation in

MeOH (75 mL), under CO in the presence of Na_2CO_3 (6.5 g, 63 mmol), to give $\text{Na}[\text{PtRh}_5(\text{CO})_{15}]$. The brown solution obtained after ca. 24 h was separated by filtration from the precipitated NaCl and NaHCO_3 and directly pyrolyzed at 80 °C at reflux under a nitrogen atmosphere for ca. 4 h. The main reaction product, $[\text{Pt}_2\text{Rh}_{11}(\text{CO})_{24}]^{3-}$, was separated as follows: methanol removal in vacuum; extraction of the residue with THF (40–50 mL) and vacuum drying; dissolution in water (26 mL), and addition of saturated KBr solution (18.5 mL); after 3 days of standing, filtration of the precipitate, washing with half-saturated KBr (10 + 10 mL), and vacuum drying. Purification of this crude $\text{K}_3[\text{Pt}_2\text{Rh}_{11}(\text{CO})_{24}]$

was done by extraction with THF (20 mL) followed by vacuum drying, dissolution in water (10 mL) and addition of NaCl (20% w/v, 7.5 mL), and, after overnight standing, filtration of a small precipitated impurity, followed by cautiously layering on the clear solution of CsCl (3% w/v, 20 mL). After complete diffusion (several weeks), the precipitated pure $\text{Cs}_3[\text{Pt}_2\text{Rh}_{11}(\text{CO})_{24}]$ was filtered and washed with CsCl (3% w/v, 10 mL). The clear mother liquor and collected washings were treated with CH_3COOH (4 mL) to give after about 3 h a fine crystalline precipitate. After the mixture was allowed to stand overnight, $\text{Cs}_4[\text{Pt}_4\text{Rh}_{18}(\text{CO})_{35}]$ was separated from the mother liquor by decantation and vacuum dried. Yields: 100–150 mg (3–4%). The product gave no hydrido signals in ^1H NMR.

(b) Synthesis as a Byproduct of the Synthesis of $[\text{Pt}_2\text{Rh}_9(\text{CO})_{22}]^{3-}$. [PPN][$\text{PtRh}_3(\text{CO})_{13}$] (1.143 g, 0.685 mmol) and [PPN] $_2$ [$\text{PtRh}_4(\text{CO})_{14}$] (1.405 g, 0.696 mmol) were dissolved under nitrogen in 25 mL of CH_3CN . The mixture was stirred at room temperature, until the IR spectrum did not change further (3–4 days). NaBPh_4 (0.733 g, 2.14 mmol) was added, and the solution was vacuum dried; the residue was redissolved in 5 mL of acetone and again vacuum dried. The residue was redissolved in water (20 mL) and filtered to remove the white precipitate of [PPN] BPh_4 , which prior to being discarded was washed with a few milliliters of water. The solution with the collected washings (final volume 28 mL) was treated with 28 mL of saturated KBr solution and stirred for 3 h and then filtered to remove this first fraction of potassium salts. The filtered solution was concentrated in vacuum to a volume of 26 mL, reaching KBr saturation, and stirred overnight. This second fraction, containing $\text{K}_3[\text{Pt}_2\text{Rh}_9(\text{CO})_{22}]$, was filtered, washed with saturated KBr, and vacuum dried. Further purification of this fraction was made by extraction with THF (20 mL) (to separate the excess KBr), followed by vacuum drying. The residue was redissolved in water (5 mL) and NaCl (20% w/v, 5 mL) and stirred overnight; this induced precipitation of a small amount of product, which was recovered by filtration and vacuum-dried. This precipitate was extracted with THF (5 mL) to give a solution which was evaporated to dryness in vacuum and the residue redissolved in MeOH (2 mL); cautious layering of a solution of NEt_4Br in 2-propanol (3 mg/mL) yielded, when the diffusion was completed, crystals which did not show a diffraction pattern. Further recrystallization from acetone/2-propanol yielded a few milligrams (10–20 mg, ca. 1%) of the acetone-solvated $[\text{NEt}_4]_4[\text{Pt}_4\text{Rh}_{18}(\text{CO})_{35}]\cdot\text{acetone}$, in crystals suitable for X-ray diffraction.

X-ray Analysis. A summary of crystal data is reported in Table II. A crystal sample of $0.35 \times 0.30 \times 0.20$ mm was mounted, on a glass fiber in air at room temperature, on an Enraf Nonius CAD4 diffractometer;

graphite-monochromatized Mo $K\alpha$ radiation was used with the generator operated at 55 kV and 25 mA. The cell parameters and the orientation matrix were obtained from a least-squares refinement of the setting angles of 25 randomly distributed intense reflections having $16 < 2\theta < 25^\circ$. The intensity data were collected using the ω -scan technique within the limits $6 < 2\theta < 50^\circ$, in the $+h, +k, +l$ octant. A variable scan speed (from 1 to $20^\circ/\text{min}$) and a variable scan range ($0.9 + 0.35 \tan \theta$) were used, with a 25% extension at each side of the peaks for background determination. Maximum time per scan was 50 s. The monitoring of the intensity of three intense reflections allowed correction for crystal decay, which was estimated about 13% at the end of the data collection. Lorentz, polarization, and absorption corrections were applied. The latter was applied to the reduced intensities based on ψ scans ($\psi = 0\text{--}360^\circ$, every 10°)¹⁶ of three reflections having χ values close to 90° ; the minimum relative transmission factor was 0.41.

The structure was solved by direct methods and conventional difference Fourier techniques and refined with full-matrix least-squares methods on the basis of 4765 independent reflections having $I > 2\sigma(I)$; anisotropic temperature factors were assigned to all metal atoms; the hydrogen atom contributions were neglected. Scattering factors for neutral atoms were taken from the SDP package database;¹⁷ anomalous scattering factors were taken from ref 18. The handedness of the crystal was determined by refining the two enantiomeric models. The final conventional agreement indices R and R_w were 0.043 and 0.044, respectively, for the best enantiomer, while the other gave $R = 0.071$ and $R_w = 0.079$. The final difference Fourier map showed a maximum peak of $1.19 \text{ e}/\text{\AA}^3$ in proximity of the Pt3 atom. All computations were performed on a PDP 11/73 microcomputer using the SDP package.¹⁷ The final positional parameters are given in Table III.

Supplementary Material Available: Listings of crystal data (Table S1), atomic coordinates and isotropic thermal parameters (Table S2), anisotropic thermal parameters (Table S3), and bond distances and angles (Table S4) (24 pages); a listing of observed and calculated structure factor moduli (Table S5) (33 pages). Ordering information is given on any current masthead page.

- (16) North, A. C.; Phillips, D. C.; Scott Mathews, F. *Acta Crystallogr.* **1968**, *A24*, 351.
 (17) Frenz, B. A. and Associates. SDP Plus Version 1.0, Enraf Nonius, 1980.
 (18) Cromer, D. T. *International Tables for X-Ray Crystallography*; Kynoch Press: Birmingham, England 1974; Vol. 4, Tables 2.3.1.

Additions and Corrections

1991, Volume 30

Fausto Calderazzo,* Alberto Juris, Rinaldo Poli, and Fausto Ungari: Reactivity of Molecules Containing Element–Element Bonds. 2. Transition Elements.

Page 1276. In Table II, the correct carbonyl stretching vibrations of $\text{CrCp}(\text{AsPh}_2)(\text{CO})_3$ are as follows (cm^{-1} ; printed values in parentheses): 1998 s (1988 s), 1934 m (1934 m), 1929 s (1989 s).—Fausto Calderazzo

Antonio Belforte, Fausto Calderazzo,* Ulli Englert, and Joachim Strähle: Deoxygenation of Carbon Dioxide to Diethylformamide in the $\text{Zn}/\text{HNEt}_2/\text{CO}_2$ System. Crystal and Molecular Structure of $[\text{Zn}_4\text{O}(\text{O}_2\text{CNEt}_2)_6]$.

Pages 3780 and 3781. The last line of text on p 3780 and the first line on p 3781 should be modified as follows: "The X-ray crystal structure is available for $\text{Zn}_4\text{O}(\text{O}_2\text{CMe})_6$,^{24a,b} whose absorption and emission spectra were recently described;^{24c} Reference 24 should be modified as follows: (a) Koyama, H.; Saito, Y. *Bull. Chem. Soc. Jpn.* **1954**, *27*, 112. (b) Hiltunen, L.; Leskelä, M.; Mäkelä, M.; Niinistö, L. *Acta Chem. Scand.* **1987**, *A41*, 548. (c) Kunkely, H.; Vogler, A. *J. Chem. Soc., Chem. Commun.* **1990**, 1204.—Fausto Calderazzo